ACS Sustainable Resource Management
Open Access

pubs.acs.org/acssrm
Article

Environmental Applications of Acid-Leached Residue Obtained during Lanthanum Recovery from Spent Cracking Catalyst

Inna Kozlovskaya* and Valentin Romanovski*

Cite This: ACS Sustain. Resour. Manag. 2026, 3, 1205−1215
Read Online

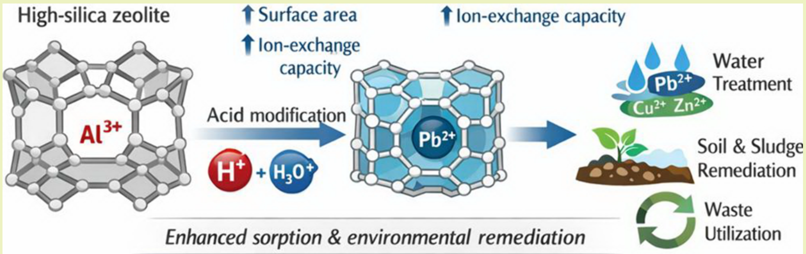

ABSTRACT: Lanthanum is widely used as a structural and textural promoter in zeolite-containing FCC catalysts. This work investigates the structural, textural, and sorption properties of the solid residue formed after acid leaching of lanthanum from spent petroleum hydrocarbon cracking catalyst. It is shown that nitric and sulfuric acids treatment aimed at extracting the rare earth element leads to significant changes in the chemical composition and surface characteristics of the residual material, while the crystalline Y-type zeolite framework is preserved. The aluminum content in the solid residue decreases from 26.8 to 14.0−15.3 wt %, while the relative proportion of silicon increases to 30.4−33.7 wt.%, indicating preferential dealumination of the amorphous matrix. The specific surface area of the material increases from 89 to 107−112 m^2/g when treated with nitric acid and to 118–120 m^2/g when using sulfuric acid, and the total pore volume increases by 21–60%. The formation of additional mesoporosity in the range of 1.5−5 nm contributes to improved sorption characteristics. The practical sorption capacity for Fe(III), Cu(II), Zn(II), and NH_4^+ ions increases by 1.5−1.8 times compared to the initial catalyst. The results show that the solid residue after lanthanum extraction is not an inert waste, but a functional sorption material comparable in characteristics to low-cost mineral sorbents and promising for environmental applications.

KEYWORDS: *spent cracking catalyst, acid leaching, solid residue, sorption properties, zeolite y*

1. INTRODUCTION

In the context of implementing the UN Sustainable Development Goals (SDGs), primarily SDG 6 "Clean Water and Sanitation" and SDG 12 "Responsible Consumption and Production," technologies aimed at simultaneously purifying contaminated water and recycling industrial waste are becoming particularly relevant.[1−4]

The use of zeolites and zeolite-containing materials in sorption processes for the purification and concentration of pollutants is one of the steadily developing areas of materials science and environmental chemistry.[5,6] The widespread use of these materials is due to the peculiarities of their aluminum- and silicon-oxygen framework, which has an excess negative charge compensated by cations of alkali, alkaline earth, and rare earth elements. This structure determines the high ion-exchange and sorption capacity of zeolites, as well as their selectivity toward a wide range of inorganic ions.

The literature shows[7−9] that zeolites exhibit pronounced selectivity toward Pb, Mn, Cr, Cs, Sr, Co, Cd, Cu, Ag, Au, Fe, and Zn ions, while the sorption capacity values, depending on the type of zeolite, modification conditions, and the nature of the adsorbate, vary in the range from 0.05 to 4.5 mg·eq/g. Zeolite-containing materials are successfully used for the extraction of heavy metals from multicomponent polymetallic solutions, including in metal concentration processes.[10,11]

In addition, there are examples of the use of such materials for purifying wastewater from ammonium ions, fluoride and sulfate ions, as well as from a number of organic compounds, including methanol and naphthalene.[12,13] The sorption properties of zeolites and zeolite-containing materials are used not only in water purification but also in binding and limiting the mobility of heavy metal ions in soils and wastewater

Received: January 22, 2026
Revised: March 25, 2026
Accepted: March 27, 2026
Published: April 1, 2026

https://doi.org/10.1021/acssusresmgt.6c00043
ACS Sustain. Resour. Manag. 2026, 3, 1205−1215

sediments,[14] as well as in the remediation of soils contaminated with petroleum products.[15,16]

To increase the efficiency of sorption, such materials are often subjected to activation or chemical modification. In particular, treatment of high-silica zeolites with solutions of mineral acids leads to partial dealumination of the structure and replacement of cations in the framework with hydronium ions or protons, which is accompanied by an increase in ion-exchange capacity and specific surface area.[17]

In this work, the spent petroleum hydrocarbon cracking catalyst is considered as a zeolite-containing material. According to the literature data, the crystalline structure of the zeolite phase in the spent catalyst corresponds to synthetic zeolite type Y, the content of which is approximately 40%.[18] Lanthanum is commonly introduced into catalysts as a structural promoter that stabilizes the zeolite framework during catalytic cracking. In recent years, spent cracking catalysts have been actively studied as a secondary raw material for the extraction of rare earth elements, primarily lanthanum. However, after acid leaching of rare earth components, a significant volume of solid residue is formed, the further use of which is often not considered or is limited to disposal.

At the same time, acid treatment of the spent catalyst can significantly alter its structural and surface characteristics, which potentially makes the solid residue a promising functional material, in particular, an adsorbent for inorganic pollutants. However, data on the physicochemical properties and sorption behavior of the residue after lanthanum extraction are presented fragmentarily in the literature and remain insufficiently studied and require systematic investigation.

The aim of this work was to investigate the structural and sorption properties of the solid residue formed after acid leaching of lanthanum from a spent cracking catalyst, as well as to assess the possibility of its further use as a sorption material for environmental protection purposes.

Unlike most studies focusing on the recovery of rare earth elements from spent catalysts, this work considers the solid residue as a potential functional sorbent material and evaluates its properties in comparison with conventional mineral sorbents.

2. MATERIALS AND METHODS

2.1. Materials and Reagents

The starting material used in this work was spent hydrocarbon cracking catalyst (SCC) obtained from an industrial catalytic cracking unit. The SCC was a fine gray powder with spherical particles. According to X-ray phase analysis data, the crystalline zeolite phase in the SCC corresponds to synthetic zeolite type Y, the proportion of which is about 40 wt %. The main components of the catalyst are aluminum and silicon oxides, as well as lanthanum compounds, which are used as a structural ionic modifier of the zeolite. Before the experiments, the SCC was used without additional thermal or chemical pretreatment.

Nitric (HNO_3, analytical grade, Sigma-Aldrich, USA) and sulfuric acid (H_2SO_4, analytical grade, Sigma-Aldrich, USA) solutions were used for acid leaching of lanthanum from the SCC. Nitric acid of "chemically pure" grade (mass fraction of HNO_3 not less than 65%) and sulfuric acid of "chemically pure" grade (mass fraction of H_2SO_4 not less than 96%) were used. Working solutions of acids with a given molar concentration were prepared by diluting concentrated acids with distilled water immediately before use.

Distilled water meeting the requirements of analytical purity was used to wash the solid residue after acid treatment. The separation of the solid and liquid phases was carried out by centrifugation without the addition of flocculants or coagulants.

In the study of sorption properties, aqueous solutions of iron(III), copper(II), zinc, and ammonium salts were used as model pollutants. Solutions of iron(III) ions were prepared from iron(III) chloride hexahydrate $FeCl_3 \cdot 6H_2O$ (analytical grade, Sigma-Aldrich, USA), copper(II) ions from copper(II) sulfate pentahydrate $CuSO_4 \cdot 5H_2O$ (analytical grade, Sigma-Aldrich, USA), zinc ions from zinc chloride $ZnCl_2$ (chemically pure grade, Sigma-Aldrich, USA), and ammonium ions from ammonium chloride NH_4Cl (analytical grade, Sigma-Aldrich, USA). All salts were used without further purification. Model solutions were prepared using distilled water.

Standard reagents for photometric and titrimetric analysis were used for the analytical determination of metal ion concentrations. Iron(III) ions were determined using sulfosalicylic acid ("chemically pure"), and zinc ions using xylenol orange ("chemically pure"). Nessler's reagent ("chemically pure") was used to determine ammonium ions. The concentration of copper(II) ions was determined titrimetrically by iodometry using sodium thiosulfate and starch as an indicator, as well as by a photometric method with chloroform extraction ("pure").

Potassium bromide KBr ("chemically pure") was used to prepare tablets for recording IR spectra. All solutions and samples were prepared and analyzed at a temperature of (20 ± 2) °C.

2.2. SCC Recycling

For the processing of the rare earth concentrate, acid solutions with concentrations of 6.0−18.0 mol/L for sulfuric acid and 4.6−14.0 mol/L for nitric acid were used. Leaching experiments were performed over a range of temperatures and contact times. The optimal conditions (90 °C and 2 h) were later identified based on regression analysis of the experimental results (see Section 3.1). Single-stage leaching of lanthanum was carried out with stirring, at a solid phase (rare earth concentrates) to acid solution mass ratio of 1:2. The leaching solution was separated into a solid residue and a liquid phase using an OS-6 centrifuge for 5 min at a rotation speed of 3000 min^{-1} (separation factor 3500). The solid residue was washed with distilled water.

2.3. Samples Analysis

The shape, nature, and composition of the surface of the SCC granules after acid treatment were evaluated at a magnification of up to 1000 times using scanning electron microscopy on a JSM 5610 LV scanning electron microscope with an EDX JED 2201 JEOL elemental analysis system (Japan). Elemental analysis was performed using X-ray fluorescence spectroscopy (XRF), which is widely applied for determining the bulk chemical composition of aluminosilicate catalysts and SCC materials. The aim of the analysis was to evaluate the relative changes in elemental composition of the catalyst before and after acid treatment.

Infrared spectra in the wavenumber range 4000−500 cm^{-1} were recorded for KBr-tableted ("chemically pure") mixtures on a NEXUS Fourier transform infrared spectrometer from THERMO NICOLET. The error in determining vibration frequencies did not exceed ±2 cm^{-1}.

X-ray diffractograms of SCC after acid leaching were obtained using the powder method on a BRUKER D8 ADVANCE diffractometer with a step-by-step scanning method (with a step in angle 2θ of 0.03° and an exposure time of 3 s at each point) in the angle range 2θ from 20 to 80°. The diffractograms were interpreted using the Match program and the EVA software package (Bruker) using the ICDD PDF-2 database.

The specific surface area and specific volume of SCC and SCC after acid leaching were measured using the low-temperature nitrogen adsorption-desorption method. The samples were studied on a NOVA 2200 instrument, which allows determining the specific surface area in the range from 10 to 1000 m^2/g; the measurement principle is based on the BET method. The pore radius (rp, nm) in SCC and the solid residue after acid treatment was calculated using the Kelvin equation.

The sorption properties of SCC and the solid residue after lanthanum leaching were judged by the values of the total static exchange capacity (TSEC). Sorption was carried out under static conditions from aqueous solutions with a given concentration (concentration range from 1 to 100 mg/L, sorbent dose −0.5 g/L, temperature 20 ± 2 °C, sorption time −2 h) and wastewater samples. The sorption properties of SCC and SCC after acid leaching were studied with respect to iron (III), copper (II), zinc, and ammonium ions.

Model solutions for sorption were prepared from the corresponding salts ($FeCl_3 \cdot 6H_2O$, chemically pure; $CuSO_4 \cdot 5H_2O$, chemically pure; $ZnCl_2$, pure; $CaCl_2$, chemically pure; NH_4Cl, chemically pure) in distilled water meeting the requirements. The concentration of metal ions was determined by photometric and titrimetric methods. When studying the sorption of metal ions, the pH value of the solutions was controlled to prevent their precipitation as hydroxides. The TSEC value, mmol·eq/g, was calculated using eq 1:

$$\mathrm{TSEC} = \frac{(C_0 - C_{eq}) \cdot V}{m \cdot M_{eq}} \quad (1)$$

where C_0 and C_{eq} are the initial and equilibrium concentrations of the adsorbate in the solution, mg/L; V is the volume of the solution, L; m is the mass of the sorbent, g; and M_{eq} is the molar mass of the equivalent, mg/(mmol·eq).

Iron ions were determined using sulfosalicylic acid, and zinc ions using the xylenol orange dye. The reported values (±15% for concentrations of 1.0−5.0 mg/L and ±10% for concentrations above 5.0 mg/L) represent the standard deviation (SD) calculated from three parallel experimental samples. These values reflect the variability of the sorption experiments rather than the instrumental error of the analytical methods used for metal ion determination. The copper content in the solution was determined by direct titrimetry with iodine in the concentration range of 10−100 mg/L (titration was carried out with sodium thiosulfate in the presence of starch), and by a photometric method with chloroform (concentration range 1−5 mg/L).

Modeling of sorption isotherms. Equilibrium sorption data were analyzed using the Langmuir and Freundlich isotherm models in order to quantify the sorption capacity and to elucidate the dominant adsorption mechanisms. The Langmuir model assumes monolayer adsorption on a finite number of energetically equivalent sorption sites and neglects lateral interactions between adsorbed species. The Freundlich model is an empirical approach that accounts for surface heterogeneity and a non-uniform distribution of adsorption energies.

The Langmuir isotherm is expressed by the following equation:

$$q = q_{max} \cdot K_L \cdot C_e / (1 + K_L \cdot C_e) \quad (2)$$

where q is the equilibrium sorption capacity ($mg \cdot g^{-1}$), q_{max} is the maximum monolayer sorption capacity ($mg \cdot g^{-1}$), K_L is the Langmuir affinity constant ($L \cdot mg^{-1}$), and C_e is the equilibrium concentration of the sorbate in solution ($mg \cdot L^{-1}$).

The Langmuir parameters q_{max} and K_L were determined by nonlinear regression of the experimental $q-C_e$ data. The quality of the fit was evaluated using the coefficient of determination R^2.

The Freundlich isotherm is described by the following equation:

$$q = K_F \cdot {C_e}^{1/n} \quad (3)$$

where K_F is the Freundlich constant related to sorption capacity, $1/n$ is the heterogeneity factor reflecting the intensity of sorption, C_e and q have the same meaning as defined above.

Values of $1/n < 1$ indicate favorable sorption and increasing surface heterogeneity, whereas values of $1/n \geq 1$ suggest weak or linear adsorption behavior. Freundlich parameters were also obtained by nonlinear regression, and the fitting quality was assessed using the coefficient of determination R^2.

All isotherm parameters were obtained by nonlinear least-squares fitting of the experimental equilibrium data. The number of experimental equilibrium points used for fitting (n) corresponds to the number of concentration points constituting each isotherm. For systems where equilibrium concentrations were not directly measured, C_e values were reconstructed from mass balance using the initial concentration, solution volume, and sorbent mass. Model adequacy was assessed by comparing R^2 values and by visual inspection of the fitted curves.

The mobility of potentially toxic metals in soils was evaluated using a single-step chemical extraction approach, which is widely applied to assess the environmentally available and weakly bound metal fractions. Soil samples were air-dried at room temperature, homogenized, and sieved to a particle size <2 mm prior to analysis. A representative subsample (5.0 g) was subjected to extraction. The solid-to-liquid ratio was maintained at 1:10 (w/v). The suspension was agitated on an orbital shaker at ambient temperature (20±2 °C) for a fixed extraction time (1 h), ensuring sufficient contact between the soil matrix and the extracting solution. After extraction, the suspension was separated by centrifugation, and the supernatant was filtered through a membrane filter (0.45 μm) prior to metal analysis. All extractions were performed in duplicate to ensure reproducibility. Metal mobility was assessed using chelating extractants that simulate natural soil solution conditions and rhizosphere processes. Applied extractants include 0.005 M DTPA (Ca−DTPA, pH 7.3). The degree of metal mobility was expressed as a mobility factor (MF), calculated according to the following equation:

$$\mathrm{MF}(\%) = C_{mob} \cdot 100\% / C_{tot} \quad (4)$$

where C_{mob} is the concentration of the metal extracted by the selected reagent ($mg \cdot kg^{-1}$) and C_{tot} is the total metal concentration in the soil determined by complete digestion ($mg \cdot kg^{-1}$).

Metal concentrations in the extracts were determined using atomic absorption spectroscopy (AAS).

The batch mixture was prepared based on the industrial composition of an aluminosilicate frit with partial replacement of the Al_2O_3 source. The residue after acid leaching of lanthanum from the ore concentrate was used as a modifying additive, introduced in an amount of 5 wt % in excess of the basic 100% batch composition without adjusting the ratios of the main components. The batch included technical alumina (partially replaced by the additive), kaolin, quartz sand, soda, and feldspar according to the technical regulations of the ceramic products manufacturing plant. All components were pre-dried, jointly ground to a homogeneous state, and thoroughly mixed. The frit synthesis was carried out under industrial ceramic production conditions by heat treatment of the batch at a temperature of 1500 °C with an isothermal holding time of 1 h, after which the melt was subjected to the standard cooling operation for frits, forming a glassy product.

Evaluation of the acid-leached residue as a lanthanum-containing microelement additive. Laboratory and field studies were conducted to assess the effect of the acid-leached residue as a lanthanum-containing microfertilizer on plant growth and development. A sod-podzolic light loamy soil without fertilizer application was used as a control. In laboratory conditions, containers with a capacity of 2 kg of soil were used, with three replicates of the experiment. Observations were carried out for 30 days, with 100 Scots pine seeds planted in each container. Field experiments were conducted in May-October 2024 and March 2025 at a forestry enterprise (Grodno region, Belarus). Observations were carried out for 30 days, with 500 Scots pine seeds planted in each plot.

Mathematical processing of the leaching results included the construction of correlation matrices and regression equations, where X1 is the acid concentration (4.6−14.0 mol/L for HNO_3 and 6.0−18.0 mol/L for H_2SO_4), M; X2 is the leaching temperature, 20−90 °C; X3 is the leaching time, 1.0−3.0 h. Python was used for mathematical processing.

https://doi.org/10.1021/acssusresmgt.6c00043
ACS Sustain. Resour. Manag. 2026, 3, 1205−1215

3. RESULTS AND DISCUSSION

3.1. Regression-Based Assessment of Lanthanum Leaching from Spent Cracking Catalyst

Based on experimental data, partially published earlier,[19] a quantitative analysis of the influence of technological parameters of acid leaching on the degree of lanthanum extraction from spent cracking catalyst was performed (Figure 1). Regression equations describing the leaching process were obtained from the experimental data. These equations were subsequently used to determine the optimal leaching conditions for further experiments (90 °C and 2 h). The experimental dependencies (eqs 1 and 2) adequately describe the change in the degree of lanthanum extraction within the studied parameter ranges, which is confirmed by the high values of the coefficient of determination (R^2 = 0.823 for nitric acid leaching and R^2 = 0.733 for sulfuric acid leaching). The regression model for sulfuric acid leaching showed a moderate coefficient of determination (R^2 = 0.733), indicating a reasonable description of the experimental trends. It was shown that increasing the temperature is the determining factor in intensifying the process, while increasing the acid concentration and treatment time leads to a less pronounced increase in the degree of extraction. Based on the obtained regression equations, it was established that at a temperature of 90 °C and a treatment duration of about 2 h, high values of lanthanum extraction (more than 90%) are achieved, which served as the basis for choosing these conditions in subsequent experiments and a mass ratio of solid spent cracking catalyst to acid solution equal to 1:2.

$$\begin{aligned} Y_{HNO_3} = {} & 255.311 - 9.155 \cdot X1 - 15.181 \cdot X2 - 79.752 \cdot X3 \\ & - 0.739 \cdot X1^2 + 9.298 \cdot X1 \cdot X2 + 15.222 \cdot X1 \cdot X3 \\ & - 0.779 \cdot X2^2 + 32.239 \cdot X2 \cdot X3 - 203.391 \cdot X3^2 \end{aligned} \tag{5}$$

$$\begin{aligned} Y_{H_2SO_4} = {} & 294.235 - 13.055 \cdot X1 - 32.828 \cdot X2 - 132.349 \cdot X3 \\ & - 1.614 \cdot X1^2 + 16.239 \cdot X1 \cdot X2 + 27.403 \cdot X1 \cdot X3 \\ & - 1.272 \cdot X2^2 + 46.489 \cdot X2 \cdot X3 - 279.204 \cdot X3^2 \end{aligned} \tag{6}$$

3.2. Sample Characterization

It is known that acid treatment of aluminosilicates under certain conditions leads to their dealumination;[17] therefore, the leaching of lanthanum from the SCC catalyst is accompanied by the transfer of aluminum into the solution. When using concentrated acid solutions, dealumination of both the matrix and the zeolite component of the SCC catalyst is possible. The aluminum located in the structural nodes of the zeolite, formed after the removal of lanthanum, is weakly bound to the framework, which makes its transition to the liquid phase possible during acid treatment.[17] Analysis of the initial SCC sample and the

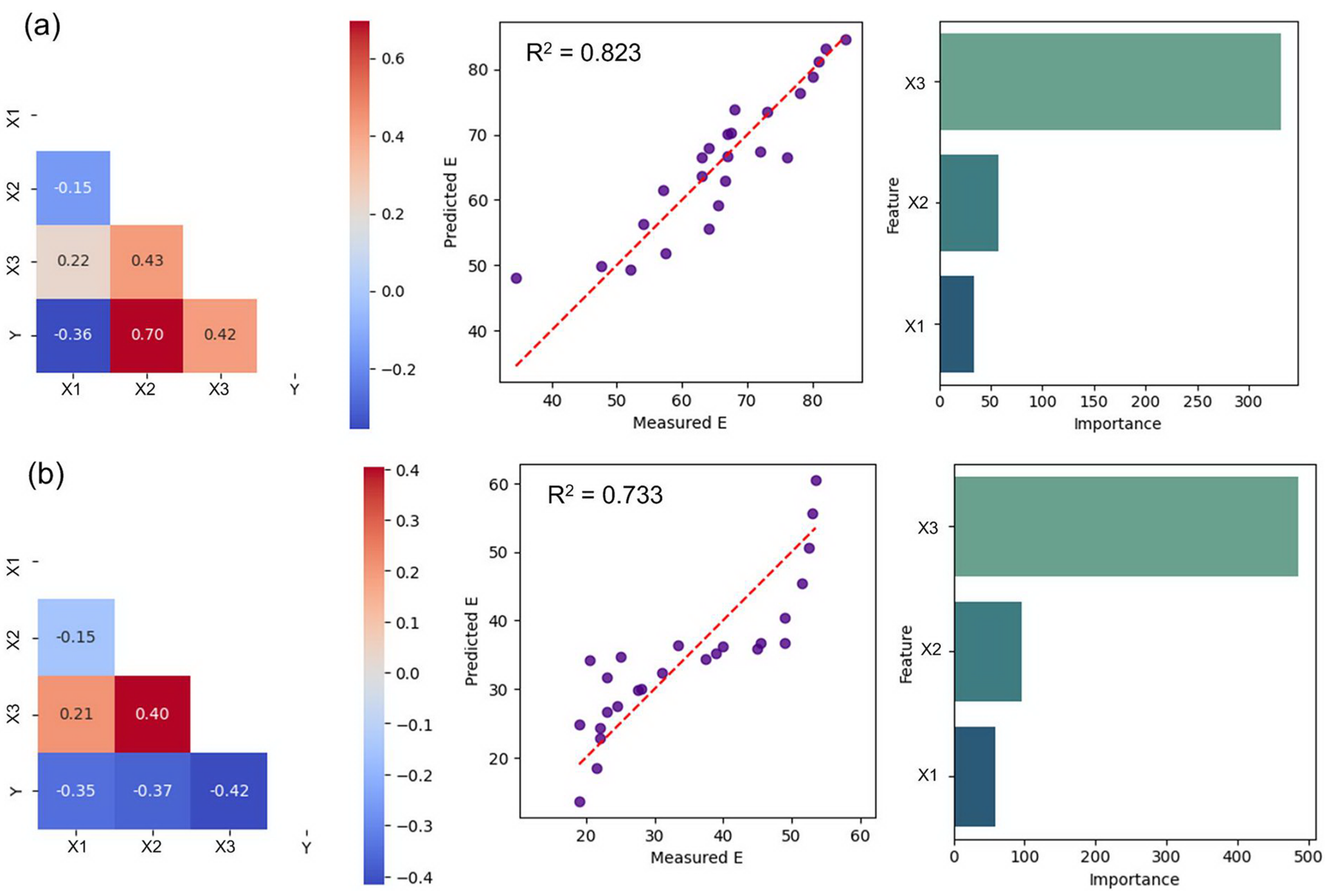

Figure 1. Pearson's correlation matrix, plots of predicted and measured values for SCC, and variable importance for nitric acid (a) and sulfuric acid (b): where X1 is the acid concentration, M; X2 is the leaching temperature, 20–90 °C; X3 is the leaching time, h.

https://doi.org/10.1021/acssusresmgt.6c00043
ACS Sustain. Resour. Manag. 2026, 3, 1205−1215

Table 1. Elemental Composition of the Initial Spent Cracking Catalyst (SCC) and Acid-Leached Residues Obtained under Different Treatment Conditions, wt%

sample	O	Al	Al_2O_3	Si	SiO_2	La	LaO_2	Na	Na_2O
SCC	49	26.8	51.4	21.3	45.3	1.8	2.21	0.6	0.9
4.6 mol/L HNO_3	51.19	15.2	32.1	32.29	64.61	1.32	3.29		
7 mol/L HNO_3	51.44	14.05	29.63	33.73	68.45	0.77	1.92		
6 mol/L H_2SO_4	51.07	15.34	32.33	32	63.86	1.28	3.19	0.31	0.63
9 mol/l H_2SO_4	51.28	14.46	30.4	32.96	66.37	1.3	3.23		

acid-leached residues obtained under different leaching conditions indicates that the degree of aluminum removal depends on the acid type and treatment conditions (Table 1).

Treatment of the carbonaceous material with acid solutions leads to partial destruction of its structure, as shown in Figure 2.

To identify possible changes in the zeolite in the SCC catalyst after acid treatment, the X-ray diffraction patterns of the SCC catalyst and its samples after acid treatment were compared (Figure 3).

As the presented X-ray diffraction patterns show, treatment with acid solutions does not lead to visible changes in the zeolite framework in the SCC catalyst. This is explained by the fact that aluminum is predominantly extracted from the SCC matrix.

Changes in the composition and structure of the silicoaluminate framework of the zeolite and the matrix in the SCC after dealumination should be reflected in its IR spectrum (Figure 3). Analyzing the obtained IR spectra of the SCC samples, it can be noted that after acid leaching, there is a slight shift of the peaks in the region of 396–615 cm^{-1}, which is possibly associated with the removal of aluminum from the tetrahedral positions in the zeolite framework [17] and with the

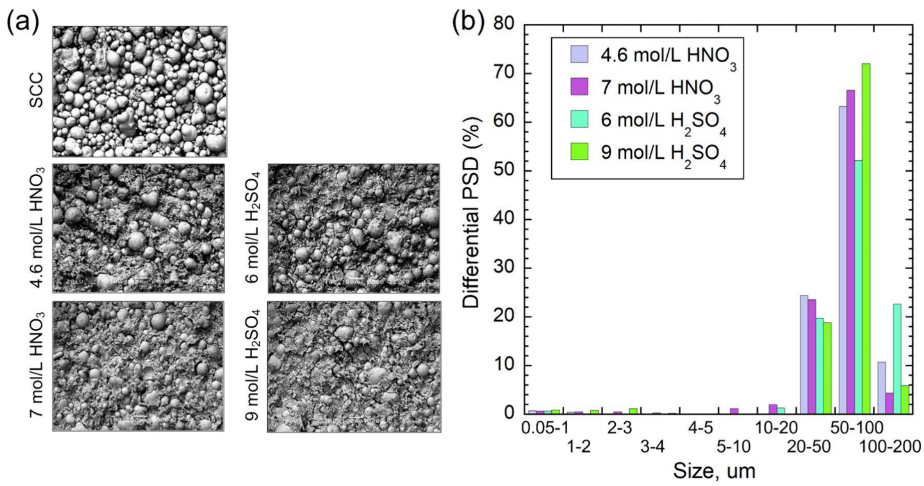

Figure 2. SEM images (a) and PSD (b) of SCC samples.

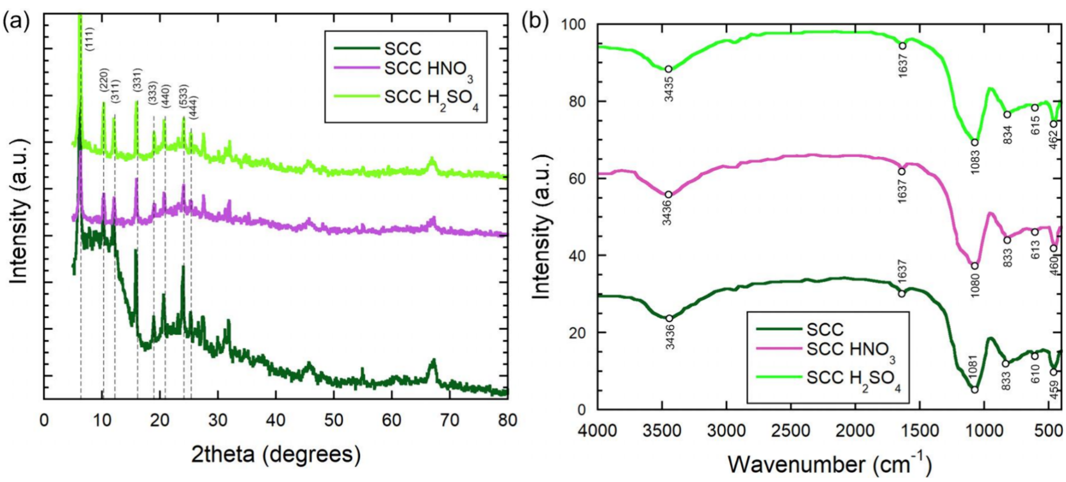

Figure 3. XRD (a) and IR spectrum (b) of SCC and SCC after leaching with nitric (7 mol/L) and sulfuric (9 mol/L) acids.

https://doi.org/10.1021/acssusresmgt.6c00043
ACS Sustain. Resour. Manag. 2026, 3, 1205−1215

dealumination of the amorphous aluminosilicate matrix. The IR spectra of the treated samples show changes in the hydroxyl region. However, the characteristic band near 3745 cm^{-1}, typically associated with isolated silanol groups formed after dealumination of zeolite frameworks, was not clearly observed. This suggests that the acid treatment did not lead to extensive formation of isolated silanol groups, although partial structural modification of the aluminosilicate framework cannot be excluded. Therefore, the IR results indicate structural modification of the catalyst rather than complete framework dealumination.

The contradictions obtained in the analysis of X-ray diffraction and IR spectroscopy data are probably explained by the fact that during dealumination of the zeolite, the oxygen positions in the aluminosilicate skeleton are preserved, and the crystalline structure of the zeolite in the SCC does not change.[17]

It has been established that acid treatment contributes to an increase in the specific surface area and specific pore volume of the SCC (Figure 4). When processed under conditions that ensure maximum lanthanum leaching, the specific surface area increases by 20.5−25.0% (to 107−112 m^2/g) when using nitric acid, and by 32−35.0% (to 118−120 m^2/g) when using sulfuric acid. The specific pore volume increases accordingly to 0.72−0.76 cm^3/g and 0.94−0.96 cm^3/g (by 21.0−27.0% and 56.0−60.0%, respectively).

It has been established that after acid treatment, the proportion of pores with a size of 1.5−5 μm increases. This fact is explained by the fact that the decationization process of the organoclay complex, accompanied by its partial dealumination, leads to a certain increase in the diameter of the effective pores and the free volume of channels and cavities in the structure of the organoclay complex.

3.3. Sorption Performance and Environmental Applicability of the Acid-Leached Residue

Acid treatment of the organic carbon concentrate leads to a significant increase in its sorption capacity for iron ions (Figure 5).

The data presented in Figure 5a indicate that acid leaching of lanthanum from the SCC is accompanied by its activation as a sorbent material. Acid activation of the amorphous and crystalline phases in the SCC is primarily associated with their dealumination. After treatment with nitric acid, the sorption capacity of SCC for iron ions increases from 0.87 mmol·eq/g to 1.7 mmol·eq/g, while with sulfuric acid, the sorption capacity reaches 3.7 mmol·eq/g.

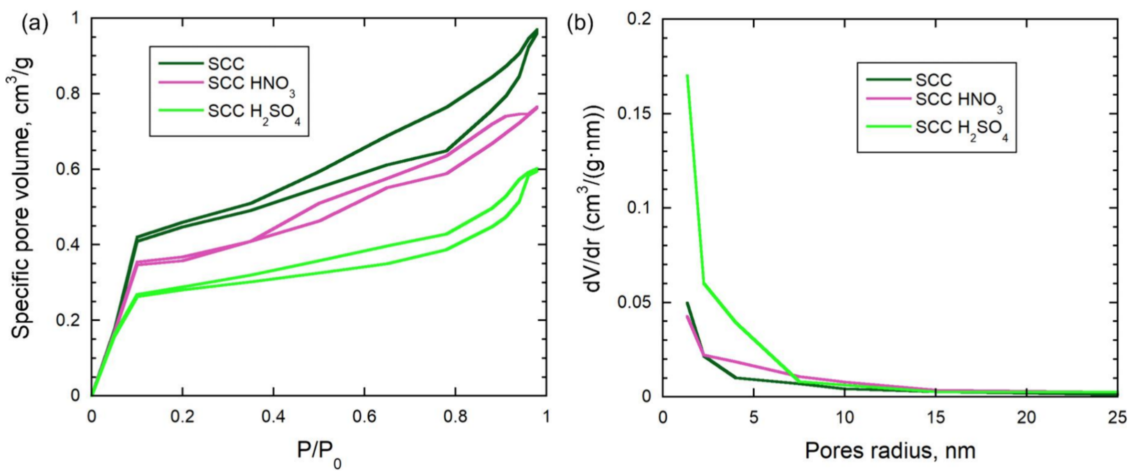

Figure 4. Nitrogen adsorption-desorption isotherm and pore size distribution of SCC, and SCC after leaching with nitric (7 mol/L) and sulfuric (9 mol/L) acids.

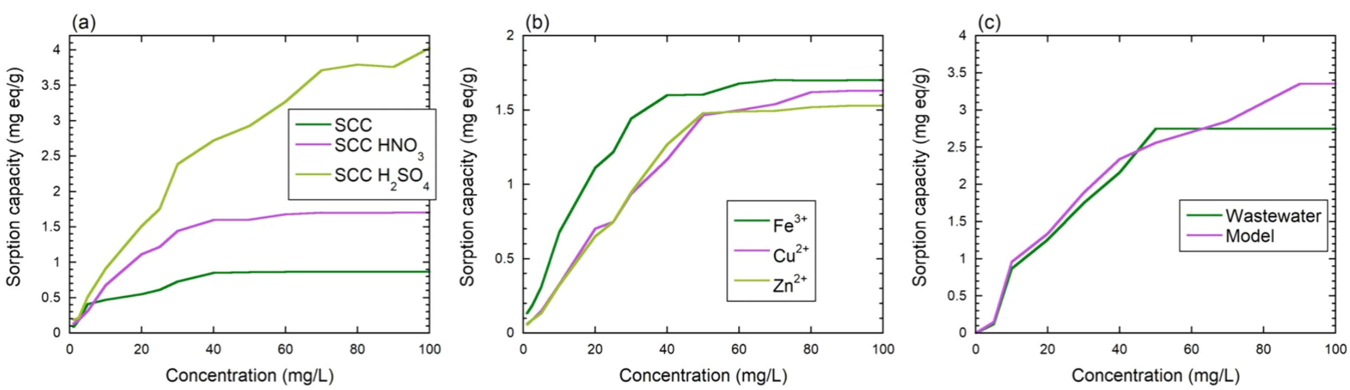

Figure 5. (a) Isotherms of iron(III) ion sorption, (b) isotherms of metal ion sorption, and (c) isotherms of ammonium ion sorption by the residue after leaching with nitric acid at room temperature (22 ± 2 °C).

https://doi.org/10.1021/acssusresmgt.6c00043
ACS Sustain. Resour. Manag. 2026, 3, 1205−1215

Table 2. Langmuir Isotherm Parameters (Nonlinear Fit)

ion	sorbent/system	n	q_{max} (mg/g)	K_L (l/mg)	R^2
Fe^{3+}	initial SCC	14	16.03	0.36213	0.854
Fe^{3+}	residue after HNO_3	13	52.89	0.09923	0.775
Fe^{3+}	residue after H_2SO_4	12	79.18	0.16806	0.923
Cu^{2+}	initial SCC	15	21.47	0.03289	0.934
Cu^{2+}	residue after HNO_3	Langmuir parameters not reported due to poor model fit			
Cu^{2+}	residue after H_2SO_4	12	182.00	0.10008	0.810
Zn^{2+}	initial SCC	15	22.15	0.09725	0.970
Zn^{2+}	residue after HNO_3	14	58.51	0.09424	0.920
Zn^{2+}	residue after H_2SO_4	15	64.64	0.06155	0.919
NH_4^+	model solution (HNO_3 residue)	7	228.04	0.00276	0.971
NH_4^+	industrial wastewater (HNO_3 residue)	9	61.46	0.08967	0.837

Comparison of the sorption properties of SCC before and after leaching with nitric acid solution for iron, copper, and zinc ions shows a significant increase (Figure 5b). The TSEC values were for iron (III) ions − 1.7 ± 0.05 mmol·eq/g (31.6 mg/g), copper (II) − 1.6 ± 0.05 mmol·eq/g (50.8 mg/g), and zinc − 1.5 ± 0.05 mmol·eq/g (51 mg/g). The highest TSEC value for Fe^{3+} is possibly explained by the fact that in the case of ions with different charges, their sorption increases with increasing ion charge. Ions with the same charge (Cu^{2+}, Zn^{2+}) are sorbed better the larger the ion radius, since a larger ion is less hydrated. The Langmuir and Freundlich parameters listed in Tables 2 and 3 indicate predominantly monolayer adsorption on heterogeneous sorption sites formed during the acid treatment.

Isotherm modeling supports the quantitative trends observed in Figure 5a−c. It should be noted that the Langmuir parameter q_{max} represents the theoretical maximum sorption capacity derived from model fitting and may differ from experimentally observed sorption capacities. For Zn(II) sorption, the Langmuir model provides an excellent fit ($R^2 \approx 0.92$−0.97 across the investigated materials), consistent with uptake dominated by a finite number of ion-exchange sites. For Cu^{2+} sorption on the nitric acid-treated residue, the Langmuir model produced unrealistic parameter values (extremely large q_{max} and near-zero K_l). This indicates that the Langmuir model does not adequately describe the sorption behavior for this system. Therefore, Langmuir parameters are not considered reliable and are not reported. This behavior may indicate heterogeneous adsorption sites or multilayer sorption processes that deviate from the assumptions of the Langmuir model. For Fe(III), both models describe the data well; however, the best fits are obtained for the sulfuric-acid residue ($R^2_L \approx 0.923$; $R^2_F \approx 0.944$), in agreement with the strong activation reflected by the increased TSEC. For Cu(II), sulfuric-acid treatment yields high capacities and good Langmuir agreement ($R^2_L \approx 0.810$), implying a combination of ion exchange and surface complexation on newly generated sites. In the case of Cu(II) for the nitric-acid residue, the presence of a high-capacity point at elevated concentration results in a poorly constrained Langmuir q_{max} (large extrapolated value), indicating that saturation is not fully reached within the investigated concentration range and that heterogeneous site energies may contribute; accordingly, Freundlich fitting provides a complementary description.

Table 3. Freundlich Isotherm Parameters (Nonlinear Fit)

ion	sorbent/system	n	K_F	$1/n$	R^2
Fe^{3+}	initial SCC	14	6.057	0.237	0.925
Fe^{3+}	residue after HNO_3	13	5.892	0.636	0.755
Fe^{3+}	residue after H_2SO_4	12	22.142	0.310	0.944
Cu^{2+}	initial SCC	15	2.926	0.369	0.878
Cu^{2+}	residue after HNO_3	14	2.494	0.815	0.851
Cu^{2+}	residue after H_2SO_4	12	38.711	0.324	0.631
Zn^{2+}	initial SCC	15	5.588	0.283	0.836
Zn^{2+}	residue after HNO_3	14	14.254	0.289	0.715
Zn^{2+}	residue after H_2SO_4	15	11.062	0.353	0.757
NH_4^+	model solution (HNO_3 residue)	7	0.846	0.882	0.964
NH_4^+	industrial wastewater (HNO_3 residue)	9	12.584	0.348	0.763

For NH_4^+ uptake, both Langmuir and Freundlich models adequately describe the model solution data ($R^2_L \approx 0.971$; $R^2_F \approx 0.964$), while the industrial wastewater dataset shows lower correlation due to matrix effects and competitive sorption (Tables 2 and 3). The observed decrease of TSEC from 3.35 mmol·eq/g (60.4 mg/g) in model solution to 2.75 mmol·eq/g (49.6 mg/g) in wastewater (≈18% reduction) is consistent with competition from Ca^{2+}/Mg^{2+} and increased ionic strength but still confirms the practical applicability of the material for ammonium removal in real effluents. The isotherm parameters generated from the model fit support our hypothesis that acid leaching can be applied to SCC in order to create an inorganic sorbent that exhibits predictable equilibrium characteristics as well as much higher metal ion adsorption capabilities compared to untreated forms of SCC. The activation via sulfuric acid allows for maximum activation of Sorbents toward iron and copper ions while using nitric acid yields an activated material that has the dual advantage of being effective against both metal ions and ammonium even in the wastewater environment. The obtained values of sorption capacity for ammonium sorption and metal cation sorption show similarities to previously reported values of zeolite-based inorganic sorbents and indicate that this new form of inorganic sorbent has a more competitive capability for both ammonium removal and metal cation removal (refer to Table 4).

Based on the results obtained, two brands of sorbent derived from activated carbon were proposed. Their characteristics, in accordance with the developed technical specifications "Sorbent for water purification" TU BY 100354659.102-2014, are presented in Table 5.

The total sorption capacity (TSEC) of the sorbent obtained from SCC for ammonium ions (sorption from model solutions) reaches 3.35 ± 0.05 mmol·eq/g (60.4 mg/g) of sorbent

https://doi.org/10.1021/acssusresmgt.6c00043
ACS Sustain. Resour. Manag. 2026, 3, 1205−1215

Table 4. Comparison of Sorption Performance of the Acid-Leached SCC Residue with Selected Zeolite-Based Sorbents Reported in the Literature

sorbent	target ion	matrix / conditions	sorption capacity (mg/g)	reference
natural clinoptilolite	NH_4^+	model solution, batch	9.8−16.3	20
natural clinoptilolite	NH_4^+	wastewater, batch	12−20	8
modified natural zeolite (acid / ultrasound treated)	NH_4^+	model solution, batch	≈140	21
diatomite-based X-type zeolite	Cu^{2+}	isotherms, 323 K	146	22
diatomite-based X-type zeolite	Zn^{2+}	isotherms, 323 K	195	22
acid-leached SCC residue (this work)	NH_4^+	model solution, batch	≈60.4	this work (Figure 6)
acid-leached SCC residue (this work)	NH_4^+	real wastewater	≈49.6	this work (Figure 6)
acid-leached SCC residue (this work)	Cu^{2+}	isotherms to 200 mg/L	≈152	this work (Figure 5)
acid-leached SCC residue (this work)	Zn^{2+}	isotherms	≈51	this work (Figure 5)

Table 5. Characteristics of the Sorbent from the SCC

parameter	SCC (AKV-1 grade)	SCC after nitric acid leaching (AKV-2 grade)
content of fraction larger than 200 μm, not more than %	10	
bulk density, g/cm^3	0.65−0.95	
total static exchange capacity	0.5	1.0
(for Fe^{3+} ions), mg-eq/g, not less than	0.7−0.9	
specific pore volume, cm^3/g	100−140	
specific surface area, m^2/g	5.5−6.5	
pH of aqueous extract	the powder is light gray in color	

(Figure 5c). The study also included research on the purification of wastewater from a woodworking enterprise, generated during the washing of filters in the production of urea-formaldehyde resins, from ammonium nitrogen. The sorption capacity of the sorbent for NH_4^+ decreases slightly, reaching 2.75 ± 0.05 mmol·eq/g (49.6 mg/g). This decrease in sorption capacity when using wastewater is explained by the fact that, simultaneously with ammonium ions, calcium and magnesium ions are also partially removed from the wash water.

A promising application of the sorbent, which does not require regeneration, is its use as a substitute for synthetic zeolites to bind and limit the mobility of heavy metals in soil and wastewater sludge. Experimental studies have been conducted on limiting the mobility (fixation) of heavy metals (cadmium, lead, nickel, and copper) using the obtained sorbent (Figure 6).

It has been established that the addition of a fixing material to excess activated sludge results in the binding of a portion of the metals. Up to 68.7% of copper, up to 53.7% of nickel, and up to 84.8% and 54.5% of cadmium and lead, respectively, were bound by the immobilizing material. The obtained values are comparable to or exceed published data for mineral and sludge-based amendments used at significantly higher doses (Table 6). The decrease in the effectiveness of limiting metal mobility when the sorbent dose is increased above 50 g/L is due to the enlargement of its particles and a sharp increase in the sedimentation rate, as a result of which the necessary interaction between the sorbent and the sludge is not ensured.

Tests were conducted on the use of the residue after acid leaching of lanthanum from rare earth concentrates, with the aim of partially replacing technical alumina in the frit composition at an industrial plant. In addition to the substituted

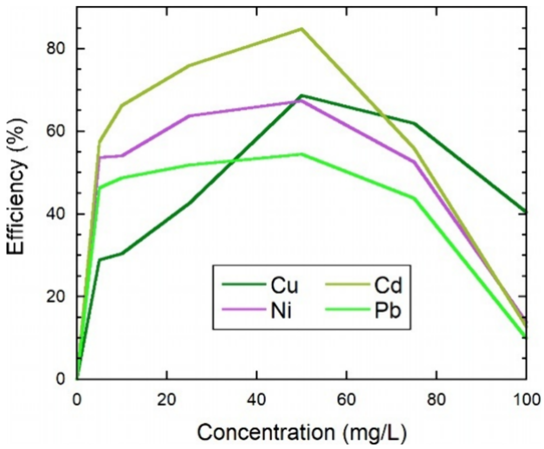

Figure 6. Effectiveness of limiting the mobility of heavy metals in excess activated sludge at different sorbent doses.

technical alumina, the frit mixture included kaolin, quartz sand, soda, and feldspar. The initial components were thoroughly ground, mixed, and subjected to heat treatment at a temperature of 1500 °C for 1 h. As a result, a frit was obtained that, in terms of its technological and physicochemical properties, fully meets the requirements for frits according to the company's technological regulations (Table 7).

3.4. Evaluation of the Acid-Leached Residue as a Lanthanum-Containing Microelement Additive

To evaluate the potential environmental compatibility of the treated catalyst residues, a preliminary phytotest was performed using Scots pine (*Pinus sylvestris*). The purpose of this experiment was not to conduct a comprehensive agronomic assessment, but rather to obtain an indicative evaluation of the possible effects of the treated material on plant growth. The solid residue after treatment with nitric acid contains lanthanum that is not incorporated into its structure, making it possible to introduce it into the soil as a trace element supplement. The lanthanum content in the solid residue is comparable to that in a slow-release micronutrient fertilizer, which consists of zeolite impregnated with lanthanum salts. Both the solid residue after acid leaching of the spent cracking catalyst and the product obtained by treating natural zeolite with lanthanum compounds from the spent catalyst can be used as a trace element supplement. As shown in publications,[25] lanthanum has a positive

https://doi.org/10.1021/acssusresmgt.6c00043
ACS Sustain. Resour. Manag. 2026, 3, 1205−1215

Table 6. Comparison of Heavy Metal Immobilization Efficiency in Excess Activated Sludge Using Different Amendments

amendment / sorbent	matrix	dose of sorbent	method for mobility assessment	immobilization efficiency	reference
FA- or CS-based stabilizers (biochar precursors)	sewage sludge-derived material	1–4% (w/w)	DTPA, $CaCl_2$, BCR fractionation	54–68% (FA); 68–92% (CS) for Zn, Pb, Cd, Ni	23
natural zeolite amendment	contaminated soil (mechanistic analogue)	5–10% (w/w)	BCR F1 (exchangeable fraction)	18–46% 30 d; 22–69% 90 d, max for Pb	24
acid-leached SCC residue (this work)	excess activated sludge	40 mg/L	decrease of mobile metal fraction	Cu: 68.7%; Ni: 53.7%; Cd: 84.8%; Pb: 54.5%	this work

Table 7. Comparison of the Physicochemical and Technological Parameters of the Experimental Frit with the Addition of 5% SCC Residue and the Regulatory Requirements for Frits

parameter	experienced frit (5% excess of total alkali content above 100%)	regulatory requirements for this type of frit:
frit type	aluminosilicate glaze	aluminosilicate
mass fraction of Al_2O_3, %	within the normative range	12–18
mass fraction of SiO_2, %	within the normative range	55–65
alkali oxides ($Na_2O + K_2O$), %	complies with the standard	6–12
alkaline earth oxides (CaO + MgO), %	complies with the standard	7–14
Fe_2O_3 content, %	≤ normative value	≤0.5
softening point temperature, °C	720–760	700–780
melting temperature, °C	1400–1500	1350–1500
melt viscosity	ensures uniform melting and glass phase formation	must ensure glaze application processability
coefficient of thermal expansion, $\times 10^{-6}$ K^{-1}	6.8–7.4	6.5–7.5
structural homogeneity	vitreous, without crystalline inclusions	homogeneous
frit color	light, without discoloration	light / colorless
chemical resistance	meets the requirements	meets the requirements for glaze frits
compatibility with ceramic body	confirmed	mandatory
technological applicability	confirmed	approved for use

effect on plant growth. Laboratory and field studies were conducted to assess the effect of the spent cracking catalyst as a lanthanum-containing micronutrient fertilizer on plant growth and development. A sod-podzolic light loamy soil without fertilizer application was used as a control. The dose of lanthanum applied to the soil was based on literature data.[26] The results of studies on the effect of lanthanum on the growth and development of Scots pine (Figure 7a,b) reflect the positive effect of using the trace element supplement from the spent cracking catalyst at various application rates.

The results presented in Figure 7 indicate that the addition of the treated residues did not inhibit the growth of Scots pine seedlings. In several treatments, a tendency toward increased plant growth compared with the control was observed. However, given the exploratory nature of the phytotest, these results should be interpreted as preliminary. Such effects are consistent with previously reported observations that aluminosilicate materials, including zeolite-containing residues, may improve soil properties through enhanced water retention, cation exchange capacity, and gradual nutrient release. In laboratory conditions, the addition of a trace element supplement derived from spent cracking catalyst increased seed germination by 9.0% compared to the control group (which falls within the experimental error range), while in field conditions, the increase was 16.0%. The results of field experiments indicate the effective use of the supplement from spent cracking catalyst in combination with mineral fertilizers (germination reaches 84.0%). It was also established that the application of the trace element supplement obtained from spent cracking catalyst positively affects the parameters of Scots pine seedlings – an increase in the average length of the above-ground part and roots of the plants is observed, and the stem thickness increases. The most significant differences are noticeable after 10 months from the emergence of shoots (Figure 7c,d).

4. CONCLUSIONS

This study demonstrates the possibility of comprehensive utilization of spent cracking catalyst through lanthanum extraction followed by the use of the resulting solid residue as a functional sorbent material. Acid leaching in the temperature range of 25–90 °C and treatment durations of 1–3 h enable effective lanthanum removal. Regression analysis adequately describes the dependence of lanthanum extraction on temperature for nitric and sulfuric acids ($R^2 = 0.823$ and $R^2 = 0.733$, respectively), allowing the optimal processing conditions to be identified.

Acid treatment significantly enhances the sorption properties of the catalyst residue. Sulfuric-acid leaching results in the highest sorption capacity toward metal ions, while nitric-acid treatment produces a material with more balanced properties suitable for the removal of both metal and ammonium ions. The sorption capacity toward Fe(III), Cu(II), and Zn(II) increases substantially compared with the initial catalyst, confirming the formation of new active sorption sites after acid treatment. Modeling of sorption isotherms using Langmuir and Freundlich equations indicates favorable sorption behavior and heterogeneous adsorption sites.

In addition to aqueous-phase applications, the obtained material demonstrates potential for environmental remediation. The solid residue effectively immobilizes heavy metals in activated sludge and contaminated soils, reducing the mobility of metal ions through ion-exchange and surface complexation

https://doi.org/10.1021/acssusresmgt.6c00043
ACS Sustain. Resour. Manag. 2026, 3, 1205–1215

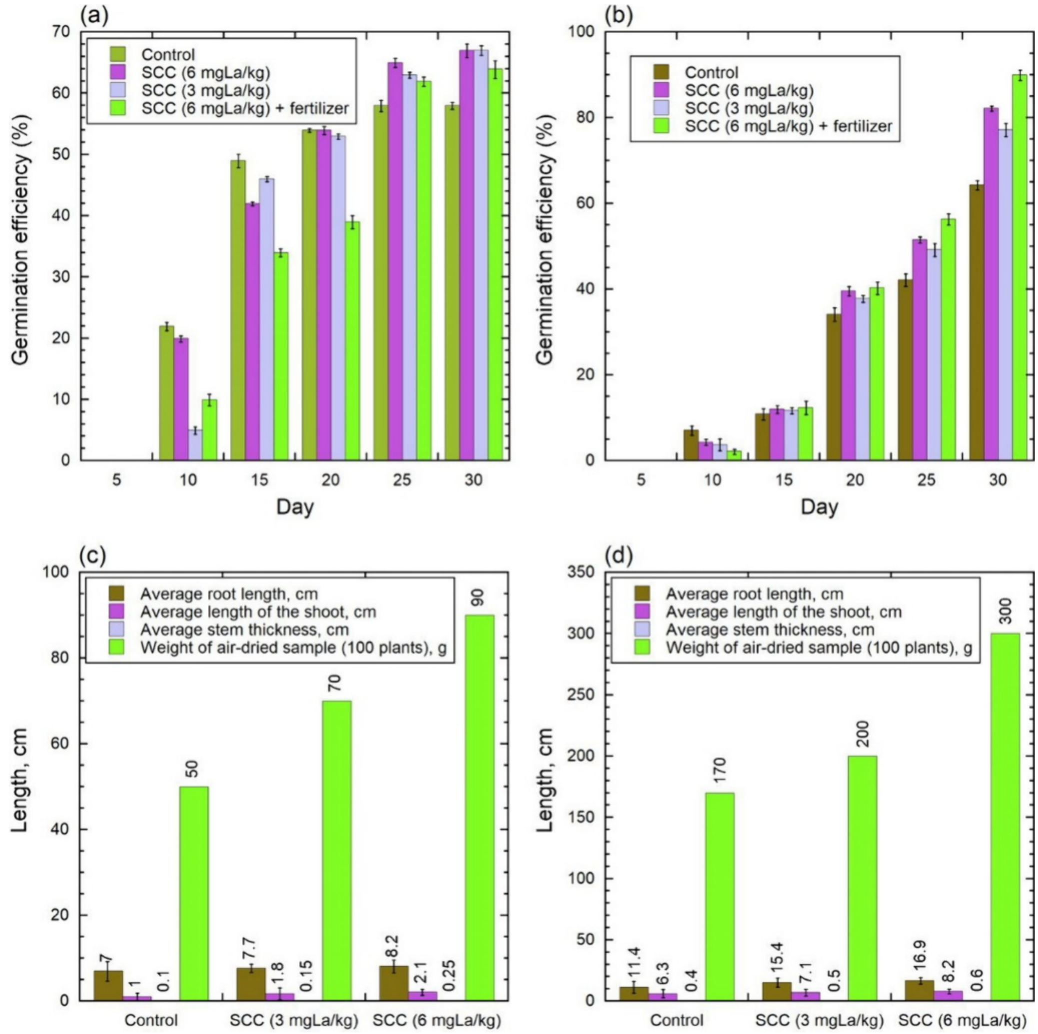

Figure 7. Germination rate of Scots pine seeds with the addition of a microelement supplement from an organic-mineral complex under laboratory conditions (a) and in field conditions (b). Parameters of Scots pine after shoot emergence: 2 weeks after shoot emergence (c); 10 months after shoot emergence (d).

mechanisms. Preliminary phytotests also indicate that the material does not inhibit Scots pine growth and may exhibit beneficial effects under the studied conditions.

Overall, the results suggest that acid-treated residues of spent cracking catalysts can be considered promising sorbent materials for environmental applications, while simultaneously enabling the recovery of valuable components such as lanthanum.

■ ASSOCIATED CONTENT

Data Availability Statement

All data, models, and code generated or used during the study appear in the submitted article.

■ AUTHOR INFORMATION

Corresponding Authors

Inna Kozlovskaya – *Department of Industrial Ecology, Belarusian State Technological University, Sverdlova, 13a, Minsk 220006, Belarus;*
Email: kozlovskayainnay@gmail.com

Valentin Romanovski – *Department of Materials Science and Engineering, University of Virginia, Charlottesville, Virginia 22904, USA;* orcid.org/0000-0003-1741-0316;
Email: rvd9ar@virginia.edu

Complete contact information is available at:
https://pubs.acs.org/doi/10.1021/acssusresmgt.6c00043

Author Contributions

I.K.: Formal analysis, data curation, validation, investigation, methodology, writing—original draft, writing—review & editing. V.R.: Formal analysis, data curation, validation, investigation, visualization, writing—original draft, writing—review & editing.

Notes

The authors declare no competing financial interest.

■ REFERENCES

(1) Romanovski, V.; Harelaya, A.; Wang, H.; Moskovskikh, D. Iron-Based Adsorbents Derived from Groundwater Deferrization Sludge

https://doi.org/10.1021/acssusresmgt.6c00043
ACS Sustain. Resour. Manag. 2026, 3, 1205–1215

for Spent Oil Removal from Aqueous Media. *ACS Environ. Au* **2026**, *6*, 154–168.
(2) Romanovski, V.; Kulichik, D.; Periakaruppan, R.; Palanimuthu, V.; Kulinich, N. V.; Popkov, V.; Romanovskaia, E. Multifunctional ZnFeO-based composite from iron sludge for photocatalytic degradation of azo, thiazine, anthraquinone dyes, formaldehyde and oil sorption from aqueous media. *J. Water Process Eng.* **2025**, *77*, No. 108355.
(3) Romanovski, V.; Gruzinova, V. Aggregate from Spent Ion-Exchange Resins for Petroleum Products Removal from Wastewater. *Waste Biomass Valoriz.* **2025**, 857–865.
(4) Gruzinova, V.; Romanovski, V. Optimizing Oil-Contaminated wastewater purification with polypropylene thread waste. *Waste Biomass Valoriz.* **2025**, *16* (5), 2521–2533.
(5) Wang, S.; Peng, Y. Natural zeolites as effective adsorbents in water and wastewater treatment. *Chem. Eng. J.* **2010**, *156* (1), 11–24.
(6) Bekkum, H. van, Flanigen, E. M., Jacobs, P. A., Jansen, J. C.Eds.; *Introduction to zeolite science and practice*,; Elsevier, **2001**.
(7) Misaelides, P. Application of natural zeolites in environmental remediation: A short review. *Microporous Mesoporous Mater.* **2011**, *144* (1−3), 15–18.
(8) Hedström, A. Ion exchange of ammonium in zeolites: A literature review. *J. Environ. Eng.* **2001**, *127* (8), 673–681.
(9) Barrer, R. M. *Hydrothermal chemistry of zeolites*; Academic Press, **1982**.
(10) Ramos, P.; Borojovich, E. J.; Zeiri, O.; Amar, Y.; Gottlieb, M.; et al. Zeolite performance in removal of multicomponent heavy metal contamination from wastewater. *J. Hazard. Mater.* **2023**, *457*, No. 131784.
(11) Kozera-Sucharda, B.; Gworek, B.; Kondzielski, I.; Chojnicki, J. The comparison of the efficacy of natural and synthetic aluminosilicates, including zeolites, in concurrent elimination of lead and copper from multi-component aqueous solutions. *Processes* **2021**, *9* (5), No. 812.
(12) Dehmani, Y.; et al. Adsorption of various inorganic and organic pollutants by natural and synthetic zeolites: A critical review. *Arab. J. Chem.* **2023**, *17* (1), No. 105474.
(13) Mažeikiene, A.; Valentukevičiene, M.; Rimeika, M.; Matuzevičius, A. B.; Dauknys, R. Removal of nitrates and ammonium ions from water using natural sorbent zeolite (clinoptilolite). *J. Environ. Eng. Landsc. Manag.* **2008**, *16* (1), 38–44.
(14) Singh, G.; Singhal, L. Natural zeolite as effective sorbent for immobilization of heavy metals in contaminated soil: Mechanisms and applications. *Environ. Technol. Innov.* **2020**, *19*, No. 100892.
(15) Wang, S.; Qiao, X. Remediation of petroleum-contaminated soils using natural zeolite and its modified forms: Adsorption performance and mechanisms. *J. Environ. Manage.* **2015**, *150*, 339–345.
(16) Muthu Manokar, A.; Vimala, M.; et al. Different parameters affecting the condensation rate on an active solar still—A review *Environ. Prog. Sustainable Energy* **2019**, *38* (1), 286–296.
(17) Tanirbergenova, S.; et al. Effect of Acid Treatment on the Structure of Natural Zeolite from the Shankhanai Deposit. *Processes* **2025**, *13* (9), 2896.
(18) Sposato, C.; Catizzone, E.; Blasi, A.; Forte, M.; Romanelli, A.; Morgana, M.; Migliori, M.; et al. Towards the circular economy of rare earth elements: lanthanum leaching from spent FCC catalyst by acids. *Processes* **2021**, *9* (8), 1369.
(19) Kozlovskaya, I.; Martsul, V.; Romanovski, V. Value-Added Lanthanum-Containing Products Recovered from Spent Cracking Catalyst. *ACS Sustainable Resour. Manag.* **2024**, *1* (12), 2593–2601.
(20) Wasielewski, S.; Rott, E.; Moser, H. Ammonium removal from water using natural clinoptilolite: Influence of temperature and initial concentration. *Water* **2018**, *10* (8), 1–13.
(21) Jahani, F.; Sadeghi, R.; Shakeri, M. Ultrasonic-assisted chemical modification of a natural clinoptilolite zeolite: Enhanced ammonium adsorption rate and resistance to disturbing ions. *J. Environ. Chem. Eng.* **2023**, *11* (5), No. 110354.
(22) Yao, Y.; Gao, B.; Chen, J.; Yang, L. Synthesis of X-type zeolite from diatomite for efficient removal of Cu(II) and Zn(II) from aqueous solutions. *J. Hazard. Mater.* **2021**, *403*, No. 123638.
(23) Huang, H.; Tang, J.; Gao, K.; He, R.; Zhao, H.; Werner, D. Heavy metal immobilization in contaminated soils by biochar: A review. *PLoS One* **2017**, *12* (4), No. e0176333.
(24) Cadar, O.; Paul, M.; Roman, C.; Miclean, M.; Levei, E. A. Immobilization of potentially toxic elements in contaminated soil using natural zeolite. *Appl. Sci. (Basel)* **2021**, *11* (4), No. 1681.
(25) Jia, T.; Gu, J.; Ma, M.; Song, Y. Lanthanum significantly contributes to the growth of the fine roots' morphology and phosphorus uptake efficiency by increasing the yield and quality of Glycyrrhiza uralensis taproots. *Plants* **2024**, *13* (4), 474.
(26) Kastori, R.; Putnik-Delić, M.; Maksimović, I. Lanthanum and cultivated plants. *Biol. Serbica* **2024**, *46* (1), 3–11.

https://doi.org/10.1021/acssusresmgt.6c00043
ACS Sustain. Resour. Manag. 2026, 3, 1205–1215